HHS Public Access

Author manuscript

ACS Chem Biol. Author manuscript; available in PMC 2017 July 15.

Published in final edited form as:

ACS Chem Biol. 2016 July 15; 11(7): 1880–1890. doi:10.1021/acschembio.6b00291.

ML314: A Biased Neurotensin Receptor Ligand for Methamphetamine Abuse

Larry S. Barak[‖,*], **Yushi Bai**[‖], **Sean M. Peterson**[‖], **Tama Evron**[‖], **Nikhil M. Urs**[‖], **Satyamaheshwar Peddibhotla**[‡‡], **Michael P. Hedrick**[‡], **Paul Hershberger**[‡‡], **Patrick Maloney**[‡‡], **Thomas D.Y. Chung**[‡,#], **R. M. Rodriguiz**[‖], **W.C. Wetsel**[‖], **James B. Thomas**[⊥], **Glen R. Hanson**[§,*], **Anthony B. Pinkerton**[‡,*], and **Marc G. Caron**[‖,*]

[‖]Duke University Medical Center, Durham, North Carolina 27710, United States

[‡]Conrad Prebys Center for Chemical Genomics at Sanford Burnham Prebys Medical Discovery Institute, La Jolla, California 92037, United States

[‡‡]Conrad Prebys Center for Chemical Genomics at Sanford Burnham Prebys Medical Discovery Institute, Orlando, Florida 32827, United States

[§]Department of Pharmacology and Toxicology, University of Utah, 260 S. Campus Drive, Salt Lake City, Utah 84112, United States

[⊥]RTI International, 3040 E Cornwallis Road, Durham, North Carolina 27709, United States

Abstract

Pharmacological treatment for methamphetamine addiction will provide important societal benefits. Neurotensin receptor NTR1 and dopamine receptor distributions coincide in brain areas regulating methamphetamine-associated reward, and neurotensin peptides produce behaviors opposing psychostimulants. Therefore, undesirable methamphetamine-associated activities should be treatable with druggable NTR1 agonists, but no such FDA-approved therapeutics exist. We address this limitation with proof-of-concept data for ML314, a small-molecule, brain penetrant, β-arrestin biased, NTR1 agonist. ML314 attenuates amphetamine-like hyperlocomotion in dopamine transporter knockout mice, and in C57BL/6J wild type mice it attenuates methamphetamine-induced hyperlocomotion, potentiates the psychostimulant inhibitory effects of a ghrelin antagonist, and reduces methamphetamine-associated conditioned place preference. In rats ML314 blocks methamphetamine self-administration. ML314 acts as an allosteric enhancer of

[*]Corresponding Authors: L.S.B.: phone, 01-919-684-6245. L.Barak@cell-bio.duke.edu. G.R.H.: phone, 801-581-3174. glen.hanson@hsc.utah.edu, A.B.P.: phone, 01-858-795-5320. apinkerton@sanfordburn-ham.org. M.G.C.: phone 01-919-684-5433. marc.caron@dm.-duke.edu.

[#]Current Address Mayo Clinic, Rochester MN 55905.

Author Contributions: This is a collaborative endeavor with significant contributions from multiple academic institutions and associated staff. It was initiated and designed through the NIH Molecular Libraries Initiative and in particular is the result of efforts from participating senior investigators including L.S.B., J.B.T., G.R.H., A.B.P., and M.G.C. Investigators at Duke University were primarily responsible for performing biochemical characterization studies in cellulo and animal studies with mice, investigators at Sanford-Burnham Medical Institute primarily responsible for chemistry and optimization of ML314 derivatives, and investigators at the University of Utah primarily responsible for performing animal studies in rats. All authors participated in the paper redaction and approval.

Competing Financial Interests - Patent applications relating to the chemistry of ML314 and its derivatives have been filed by the Sanford-Burnham Medical Research Institute and Duke University. The authors have no other competing financial interests related to this work.

endogenous neurotensin, unmasking stoichiometric numbers of hidden NTR1 binding sites in transfected-cell membranes or mouse striatal membranes, while additionally supporting NTR1 endocytosis in cells in the absence of NT peptide. These results indicate ML314 is a viable, preclinical lead for methamphetamine abuse treatment and support an allosteric model of G protein-coupled receptor signaling.

Graphical abstract

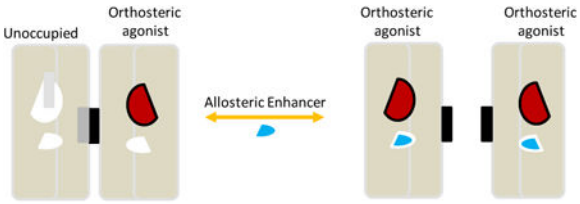

Keywords

addiction; allosteric; arrestin; dopamine; drug-abuse; GPCR; ML314; methamphetamine; neurotensin; receptor

Methamphetamine (meth) use creates an enormous social and economic burden, with complications including illness, job loss, and crime [1, 2]. Identifying drugs active in the central nervous system that counteract undesirable meth associated behaviors is a high priority that is supported by the recognition that drug addiction is a brain disorder [3, 4]. Dopamine (DA) signaling in the ventral tegmentum area (VTA) of the brain has received considerable attention for its neurobiological role in mediating the reinforcing actions of drugs of abuse and the tridecapeptide, neurotransmitter neurotensin (NT), identified over 30 years ago [5], has high affinity receptors densely expressed throughout the VTA. 6-Hydroxy-dopamine lesioning studies suggest the majority of them are located on DA neurons that are subject to NT regulation [6, 7]. NT is also a neuromodulator of DA transmission in the nucleus accumbens (NAc) and nigrastriatal pathways [8-13], and its influence on DARPP-32 phosphorylation is hypothesized as critical for the brain's response to psychostimulants [14].

Neurotensin binds two G-protein-coupled receptors (GPCRs), NTR1 and NTR2 [15-20]. This is important from a drug-development strategic perspective since GPCRs are historically druggable and signal through G protein and β-arrestin pathways that can be selectively modulated [21]. NTR1s are highly localized in specific brain regions whereas NTR2s are more widely dispersed, and the VTA and substantia nigra are the only two brain regions where significant concentrations of both receptors coexist [13, 22]. The peripheral administration of NTR1 peptide agonists produces behaviors exactly opposite the classical effects associated with psychostimulant abuse such as hyperactivity, cognitive deficits, psychotic episodes, and neurotoxicity. Importantly, NT peptides reverse meth induced hyperactivity, are cognitive enhancers [23], display antipsychotic properties in animal models, and are neuroprotective [24-26] (for a comprehensive review see [27]). In animal studies the NT peptide variant NT69L produced blockade of D-amphetamine induced locomotor activity and did

not elicit tolerance [24, 28]. Collectively, these findings support the notion that NTR1 is a valid target for treating meth abuse [1].

To date there are no FDA approved NTR1 drugs. Only a very limited number of NTR1 drugs have good central nervous system (CNS) penetration, and only the peptide NT69L and the small molecule antagonist SR142948 ever reached early clinical trials [29, 30]. Our goal to identify candidate NTR1 agonists for meth-associated addiction research via the Molecular Libraries Screening initiative led to the identification of ML314, a small molecule, brain penetrant, functionally selective β-arrestin agonist [31-36]. Here we show in vivo that ML314 is also a promising preclinical lead that reduces hyperlocomotion in mouse models of psychostimulant use, decreases conditioned place preference (CPP) in meth sensitized mice, and reduces self-administration of meth in an appropriate rat model. As part of its mechanism of action, ML314 unmasks hidden NTR1 binding sites, producing in membranes a remarkable three-fold increase in their numbers.

Results and Discussion

ML314 is brain penetrant [35], making it potentially applicable for modulating CNS behavioral phenotypes. Some synthetic, metabolically stable NT peptide analogs like PD149163 (PD) are also brain penetrant and PD in particular has demonstrated some antipsychotic-like efficacy that is mediated through CNS neurotensin receptors. In a rat model the repeated daily administration of PD produced an increase in baseline locomotor activity whereas its acute administration was shown to antagonize amphetamine's locomotor-activating ability [24]. DAT-KO mice provide a model of extracellular dopamine excess similar to what is encountered with amphetamine administration and we used these mice to compare PD to ML314 in inhibiting hyperlocomotion.

ML314 reduces locomotion in Dopamine Transporter knock-out (DAT-KO) mice

To assess the characteristic behaviors of the locomotor responses to treatment (PD, fig. 1A, and ML314, fig. 1B), the data were analyzed using a minimum number of free parameters with Lorentzian or Gaussian (amplitude, center, width, and offset) fitting models rather than by assessing point by point differences between pairs of responses at corresponding times. The fits were qualitatively very similar but the Lorentzian model was marginally better.

Each compound was administered by intraperitoneal (i.p.) injection (arrows in figures) and each showed efficacy in countering hyperlocomotion for an extended period after administration (red fitted Lorentzian curves) in comparison to vehicle controls (blue fitted Lorentzian curves). Ghrelin receptor antagonists are also being investigated for their efficacy in countering addictive behaviors [37] and we assessed ML314's ability to potentiate the efficacy of the GHSR1a antagonist YIL781. Figure 1C shows that in the DAT KO mouse, ML314 at suboptimal concentrations of 5 mg/kg combined with the ghrelin receptor antagonist YIL781 was more effective than YIL781 alone in reducing hyperlocomotion (red versus green curve).

ML314 does not affect the wire grasping ability of C57BL/6J mice

Before measuring locomotion in inbred mice, we assessed them for a loss of neuromuscular control as a measure of possible sedating effects of ML314. We assessed the ability of C57BL/6J mice to grasp and hang onto a wire for up to 60 seconds 30 and 60 minutes after 20mg/kg ML314 (i.p.) administration. There were no observed differences between vehicle (n=12) and ML314 injected mice (n=22) at either 30 or 60 minutes post treatment, and all mice successfully completed the task.

ML314 reduces hyperlocomotion and Conditioned Place Preference in C57BL/6J mice exposed to methamphetamine

The DAT-KO model results indicate that ML314 may be applicable to an amphetamine model of drug behavior in which dopamine tone is increased. We assessed this with hyperlocomotion and conditioned place preference (CPP) studies (figs. 2A-D). The locomotion data are analyzed as described above using 4 parameter fits. In the presence of 2 mg/kg meth (i.p.), mice treated with 10-30 mg/kg of ML314 had locomotion displacement curves of lower amplitude than vehicle treated ones, a reduction that corresponds to a decrease in distance traveled (figs. 2A,B, (red) vehicle vs. (blue) ML314 co-treatment). Mice conditioned to show place preference for meth had a 30% reduction in this behavior when treated with ML314 (figs. 2C, D).

ML314 reduces self-administration of methamphetamine in rats

To simulate human meth abuse, we employed a self-administration paradigm in which meth is contingently administered by rats [1, 38]. The act of contingently administering meth produces distinctive regional neurotensin responses in the brain that differ from that of animals receiving noncontingent meth and these regional alterations are related to processes of self-administration [38]. We observed that ML314 pretreatment of rats trained to self-administer meth by lever pressing (fig. 2E) significantly reduces operant behavior linked with 0.06 mg meth (i.v.) infusion per press over 4 hours from 59.1 ± 8.3 to 30.1 ± 8.7 events, whereas the behavior in rats not treated with ML314 was unchanged.

ML314 antagonizes G protein signaling

β-arrestins, as a functional consequence of their GPCR interaction, traffic with receptors to clathrin rich regions of membrane, coated pits, and endosomes. The more stable complexes concentrate in endosomes and are visible by fluorescence microscopy of β-arrestin tagged with green fluorescent protein (GFP) [39, 40]. Figure 3 provides a representative example comparing the respective abilities of NT and ML314 to translocate β-arrestin in NTR1 β-arrestin2/GFP containing U2OS cells. The induction of aggregates by ML314 (fig. 3A, right panels) is evident compared to vehicle (left panels) and is comparable to the NT peptide response (fig. 3A, middle panels). Supporting the finding that the ML314 response is mediated through the NTR1 are competition experiments in which the antagonist SR142948A blocks β-arrestin aggregate formation for the neurotensin peptide NT(8-13) [35], and at similar potency for micromolar concentrations of ML314 [35], and the related small molecule agonist ML301 (fig. 3B left) that was also synthesized for this project [34]. We have observed using an aequorin calcium reporter and a ratiometric calcium assay that ML314 is

unable to activate calcium through the NTR1 [32, 35]. Binding of ML314 to either an allosteric or overlapping orthosteric receptor site [41], however, might perturb NTR1-mediated Gq signaling (fig. 3B right panel). The data indicate that either of the two compounds, ML301 or ML314, reduces the Gq mediated calcium response of the full G protein agonist NT (8-13). ML314 is more efficacious and its behavior serves to demonstrate that while it is an agonist promoting NTR1/β-arrestin2 interactions, it functions much like a NTR1 antagonist at Gq signaling.

ML314 increases the number of NTR1 binding sites *in cellulo*

The absence of radiolabeled ML314 analogs precludes a direct assessment of its NTR1 binding characteristics. Consequently, we assessed this indirectly using ^{125}I-NT binding to NTR1 expressing membranes and the ability of ML314 to compete for ^{125}I-NT binding. Both NT and ML301 fully compete for ^{125}I-NT binding (fig. 4A). Most surprisingly, we observed a 7.5 fold increase of low picomolar ^{125}I-NT binding in the presence of ML314 rather than a displacement of radioactivity (fig. 4A). This increase also was observed in a ML314 concentration range, log(EC50) = -6.5 ± 0.45, where ML314 produces a NTR1 mediated recruitment of β-arrestin2.

Positive allosteric modulators (PAM) have already been identified for many GPCRs [42], and those that increase orthosteric ligand affinity can recapitulate some characteristics of the ML314 dose response curve in figure 4A. For this very reason, PAMs are considered desirable leads for developing new therapeutic drugs targeting CNS disorders as their efficacy depends on the endogenous ligand [42]. However, most PAMs do not increase efficacy to anywhere near the degree observed here. To investigate the source(s) of the new binding sites, particularly to rule out enhanced nonspecific binding, we measured the extent to which the labeled ligand could be displaced by cold NT in the presence of increasing ML314 concentrations (fig. 4B). The data show a dose dependent increase in the enhanced ^{125}I-NT binding that was completely displaceable to background levels. These results indicate that the binding is specific and most probably NTR1 associated.

ML314 does not increase β-arrestin activity beyond that observed with neurotensin *in cellulo*

β-arrestins bind ligand-activated G protein coupled receptors, and once bound they facilitate clathrin-mediated receptor internalization. To determine if ML314 modulated either of these processes we measured dose dependent NT-mediated NTR1 internalization using a recently developed fluorogen activated reporter assay (figs. 4C and 4D) and NT-mediated β-arrestin2-GFP recruitment using a translocation assay (fig. 4E) [43-45]. In contrast to the binding results, where ML314 increases receptor Bmax, the maximal absolute amount of endocytosed receptor is unchanged from that observed with NT alone (fig.4C). Likewise, the maximal amount of β-arrestin2-GFP recruitment is also unchanged. We did observe with 10 μM ML314, however, an expected increase in activity near zero NT concentration for both endocytosis and β-arrestin recruitment (figs. 4D and E) and a suggestion of a twofold enhancement in the EC50 for NTR1 endocytosis (fig. 4D).

ML314 increases the number of NTR1 binding sites in striatal membranes

Figure 5A compares the nonspecific binding in the presence of cold NT and the NTR1 antagonist SR142948A of ^{3}H-NT to NTR1 receptors permanently transfected into U2OS cell membranes. The equality in slopes for the non-specific binding indicates that the displaced binding sites are in all likelihood due to the overexpressed NTR1. Figure 5B shows ^{3}H-NT saturation binding of the NTR1 expressing cell membrane in the presence and absence of ML314. In the presence of ML314 we observed a 2.8 ± 0.6 fold increase in associated Bmax and a 4.8 ± 2.1 fold increase in affinity with unitary Hill slopes, indicating a lack of cooperative binding as opposed to data for reconstituted liposomal dispersed NTR1 that are assumed to be dimers [46]. To demonstrate the relevance of these results to neuronal tissue we performed ^{125}I-NT studies in striatal tissue extracts from mouse brains. Figures 5C-E demonstrate an increase in Bmax in the presence of ML314 also occurs and is similar in magnitude to that observed in tissue culture cells.

ML314 displays some intriguing pharmacological properties

As NTR1 vs NTR2 selective [33], ML314 possesses full efficacy in activating NTR1/β-arrestin interactions but almost no efficacy in activating NTR1/Gq mediated calcium signaling, thus functioning as a β-arrestin biased agonist [31, 32, 36]. It also acts like an allosteric compound at the NTR1, significantly increasing the binding of NT to the NTR1 receptor. Most significantly, it penetrates the central nervous system upon peripheral administration where it functions *in vivo* like a conventional NTR1 agonist by reducing negative behaviors in rodents modeling meth use. NT mediated NTR1 activity in the CNS is closely associated with the rewarding and motor pathways mediated by DA [47]. However, the complexity of this association has historically made it difficult to predict the *in vivo* efficacy of compounds regulating NTR1 activity [24, 30]. Thus, our promising behavioral findings that peripherally administered ML314 antagonizes hyperlocomotion in DAT-KO, meth sensitized C57B6J mice, CPP in C57B6J mice [48], and rat meth self-administration provide compelling reasons for extending ML314 studies to animal models of drug extinction and reinstatement.

The biochemical data suggest that the in vivo mechanism of action of ML314 results from a combination of G protein signaling antagonism occurring in the presence of ongoing β-arrestin activation. Our observation that the orthosteric NTR1 antagonist SR142948A blocks formation of ML314-induced β-arrestin complexes and the absence of observed ML314-mediated G protein activity at the NTR1 [35] indicate that ML314 is β-arrestin functionally selective. The increase in Bmax for NTR1/NT binding in the presence of ML314 also supports the notion that the NT binding site has at most partial identity with the ML314 site, and in this instance ML314 is acting as an allosteric modulator. However, we cannot rule out that after an ML314-induced arrestin/receptor complex forms, ML314 dissociates from the orthosteric site and is replaced by NT. A more potent and/or radioligand derivative of ML314 will be necessary to directly define the characteristics of its binding site.

While allosteric modulators are not at all unusual [42], examples of allosteric compounds that increase Bmax to the degree we observed are much rarer. Recent examples are metal ion chelators that bind the chemokine receptor CCR1 and increase the Bmax of ^{125}I-CCL3 by up to 3 fold, (see Table 2 in [49]), and the modulators Org 27569 and PSNCBAM-1 that

promote a twofold increase in saturation binding of ^{3}H-CP55940 in membranes containing the CB1, (see Table 4 in [50]). Previous observations also include an effect of changes in sodium ion concentrations from 3 to 150 mM that increase the Bmax of ^{3}H-raclopride binding to the dopamine D2 receptor in rat striatal membranes by 1.47 ± 0.05 fold [51]. Crystallographic studies with the A2A adenosine receptor indicate the allosteric effect of Na^{+} on GPCR binding is strongly regulated by an aspartic acid residue conserved in the second transmembrane domain of many GPCRs. This aspartic acid presumably regulates the high affinity state conformation between ligand, receptor and G protein[52].

Allosterism underlying ML314 changes in Bmax

Many studies support a classical model of allosterism in which proteins assemble in plasma membrane oliogomeric complexes, dimers being a minimal conformation[53-55]. For receptors in these configurations, conventional binding experiments with the endogenous ligand may underestimate total receptor expression, Bmax, if the number of receptors forming an oliogomeric receptor complex is greater than the number of functioning orthosteric binding sites in the complex in the presence of G proteins. The observed ML314-mediated Bmax increase for NTR1 strongly suggests a behavior conforming to a Monod, Wyman, and Changeux (MWC) model of allostery of protein arrays [56]. Within this picture of cooperative protein interactions and with a few additional symmetry considerations, we can construct a simple model of receptor organization that predicts allowed increases in Bmax (figure 6).

We begin by assuming that (a) the smallest functional receptor signaling unit is a protomer (which could be a monomer, dimer, or higher ordered structure), (b) the more basic allosteric signaling complexes express higher degrees of symmetry and in the most fundamental case all sites are equivalent, and (c) the breaking of symmetry in a large oliogomeric complex results in a new signaling entity. Thus, for dimer protomers (fig. 6A) in which only one site initially binds ligand, the possible observed increases in Bmax, which we term mRn, (m = number of binding sites per protomer, n = number of sides of a basic polygonal unit) are limited to a single value, namely 1R2 = 2:1. By extension, for an n-gon (n sided polygon) of these protomers 1Rn is a value from the sequence (2n):1, (2n):2,…, (2n):n (fig. 6B), and the possible choices for 1R6 are 12, 6, 4, 3, 2.4 and 2.

How array symmetry is broken further restricts allowable values of mRn. Figure 6C shows a hexamer complex of repeating dimer protomers in which symmetry is broken by linear polarized arrays of G proteins (see reference 57 figure 1a and reference 58 figure 3c respectively for these types of orderings). Multiple sites of 2 protomers perpendicular to the G protein array are unavailable and for the remaining sites all filled 1R6 equals three. Similarly, for dimer protomers with two sites bound and the same symmetry breaking configuration 2R6 equals 12:8 or 1.5. This symmetry construction offers a G-protein-based explanation for the allosteric enhancements in Bmax discussed above. For the NTR1 it agrees with observations that rhodopsin forms hexamer arrays [57], that transducin forms polarized linear arrays [58], and that arrays of rhodopsin dimer protomers signal [54]. Moreover, every protomer of an array, irrespective of initial position, has a potential to signal due to the turnover of the entire complex that is regulated by G protein coupled receptor kinase and

arrestin activities, and in the case of arrestins the stoichiometry with receptors reverts to 1:1 [59].

Biologists have had considerable success in modeling GPCR behavior by treating receptors as monomeric signaling entities. While this concept works generally well to explain logistic responses for basic biochemical assays, it fails to address fundamental questions of signal transduction concerning if and how receptors cooperatively assemble into localized or extended G-protein dependent, macromolecular arrays of signaling units. By no means are these just contemporary issues arising from current interests in receptor hetero/homo-dimerization. Martin Rodbell almost four decades ago postulated oligomeric signaling complexes composed of receptors and dynamic arrays of G proteins [60, 61]. Other than for rhodopsin, direct imaging of plasma membrane GPCR assemblies will require new or improved technologies to supplement older methods that probed signaling arrays for protein sizes but not spatial relationships [62]. Our findings here provide a pharmacologic test for evaluating oligomerization by using compounds that unmask a quantized number of receptor orthosteric binding sites presumably blocked by allosteric constraints of the signaling array.

Conclusion

Current drug treatments of GPCR-related diseases emphasize exposing orthosteric receptor-binding sites to saturating levels of agonist or antagonist drugs to correct signaling abnormalities. While these strategies can restore signaling toward their desirable ranges, they lack the regulatory subtleties provided by endogenous ligands, and in many instances lead to undesirable therapeutic consequences. Thus, drugs that affect receptor signaling in a more limited manner, for example either through preserving endogenous ligand activity or by selective downstream pathway activation, may minimize problems associated with typical pharmacotherapy. ML314 has characteristics of both a positive allosteric modulator and a β-arrestin biased agonist, but in addition it also displays antagonism for G protein signaling. This is intriguing from the perspective of a developmental drug. Allosterism and functional selectivity are clinically desirable and each alone is sufficient to serve as a basis for a new, therapeutic class of compounds.

Materials and Methods

Chemicals

YIL781, was purchased from Tocris Biosciences (Ellisville, MI). ML301 and ML314 were supplied by the Conrad Prebys Center for Chemical Genomics at the Sanford Burnham Prebys Medical Discovery Institute[34].

β-Arrestin2 Translocation Assay

U2OS cells stably expressing β-arrestin2-GFP and human neurotensin receptor 1 (NTR1) were plated at a density of (4–8) × 10^4/well in 35 mm MatTek (Ashland, MA) glass coverslip dishes. The cells were treated with 100 nM NT(8-13) or 10 μM of ML301/ML314 compound for 40 min, fixed in paraformaldehyde, and then examined on a Zeiss Axiovert 200 fluorescence microscope using a plan apochromat 40×/0.95 N.A. air objective. Images were analyzed using a wavelet algorithm to remove noise and low frequency background

fluorescence. For the antagonist inhibition assay to check the specificity of translocation, the cells were pre-treated with serial concentrations of SR142948A for 10 min, and then supplemented with 10 μM ML301 or ML314, or 5 nM NT(8-13) for another 40 min. Cells were imaged as above and the number of fluorescence objects determined.

Apo-aequorin Calcium Assay

The assay was similarly performed as described [32]. HEK293 cells were used that expressed stably transfected NTR1 and a mitochondrial membrane localized apo-aequorin calcium reporter. Suspended cells were equilibrated with 5 μM Coelenterazine H for 2 hours by shaking at 160 rpm in a dark 37°C incubator. Ten minutes prior to measurements, cells were pre-treated with vehicle or with 10 μM of ML301 or ML314. Measurements were made by injecting approximately 50,000 cells into a well of a white OptiPlate (PerkinElmer; Waltham, MA) containing a fixed concentration of the neurotensin peptide fragment NT(8-13). Luminescence was recorded for 15 seconds using a Mithras LB940 luminescence reader running MikroWin2000 software (Berthold Technologies, Oak Ridge, TN) (N = 3).

NTR1 Binding in U2OS Membranes

U2OS cell membrane assays were carried out using 15-30 μg of membrane protein per point from cells stably expressing NTR1 receptors. Briefly, NTR1-U2OS cells were grown to confluence in 150 mm dishes, washed once with cold PBS, and detached using a cell lifter in 3 ml of assay buffer (50 mM Tris, 0.1% BSA and Roche protease inhibitors, pH 7.4). The cell suspension was disrupted over ice using a Teflon® glass homogenizer. To remove tissue debris and nuclei, the resulting homogenate was centrifuged at 1000 rpm for 10 min at 4 °C. Membrane protein was collected by subsequent centrifugation at 40,000 g for 20 min at 4 °C and stored at -80 °C until use. For experiments the cell membranes were further sheared by passing them repetitively through a 25G needle (2-3 times). The membranes were first incubated with neurotensin peptide, ML301, or ML314 at the indicated concentrations for 10 min on ice. ^{125}I-NT was added to 10 pM in each well for an additional hour of incubation in ice cold buffer. Binding reactions were terminated by filtration of membranes onto glass (GF/B - Whatman) filters using a 96 channel Brandel plate harvester, and this was followed by three rapid washes with cold 50 mM Tris-HCl buffer (pH7.4). Filter disks were transferred to scintillation vials and 4 ml Bio-Safe II scintillation cocktail was added to each vial. CPM of hot neurotensin were determined using a Packard 1900TR liquid scintillation analyzer. Each experiment was repeated at least three times with repetitions occurring on separate days.

NTR1 Binding in Striatal Membranes

Striatal membranes from DAT knockout mice were prepared as described in 50 mM Tris buffer containing 5 mM EDTA, and a Roche protease inhibitor cocktail at pH 7.4 and 4° C. 100 μg/well of membrane protein was pre-incubated for 10 min at room temperature with 1 μM cold NT or 1-10 μM of ML314 with quadruplicate determinations made per point. Following the addition of hot ^{125}I-NT to each well at 10 pM, the incubations were continued for 90 additional minutes. Binding was determined as above. Protein was determined for 100 μg membrane fractions using a BCA® protein assay kit (Pierce, Rockford, IL).

Fluorogen Activated Protein Internalization Assay

The 5′-signal sequence of the leucine rich repeat G protein coupled receptor, Lgr5, and immediately following it, the single-chain antibody sequence of MarsCy1 were PCR-amplified and overlap-exchanged into the N-terminus of the human neurotensin receptor 1 (PubMed Accession number NM_002531) [44, 45]. A LI-COR Odyssey® (LI-COR Biosciences, Lincoln, NE) system in the 700 nm channel was used for scanning MarsCy1 tagged receptors stained with the plasma membrane impermeant fluorescent compound SCi1 with focal offsets adjusted to match the focal plane of the plate. SCi1 was reconstituted in ethanol with 5 % acetic acid at 78 μM and utilized at approximately 1:4000 dilution. Live cells were incubated with 20 nM SCi1 for 5 minutes and then imaged. No washing was performed unless indicated. Receptor internalization was measured with a modification of the primary assay as described [44]. In brief, U2OS cells in 100 mm plates were transiently transfected on day 0 with the NTR1 plasmid using Lipofectamine 2000 via its standard protocol (Life Technologies, Carlsbad CA) and were split into 96 well plates on day 1 in 100 μL serum free media (MEM) supplemented with 10% FBS (ThermoFisher/GIBCO, Waltham MA). On day 2 the media was replaced with MEM containing 10mM HEPES and 1% Glutamax (ThermoFisher/GIBCO). On day 3 the cells were assayed for 1 hour at 37°C in 5% CO2 by replacing the media with 75 μL of an equivalent solution also containing the drugs, and at 1 hour the plates were immediately scanned after adding 25 μL of Sci1.

Preparation of ML314 for intraperitoneal injection in mice

Solutions for rats were prepared similarly to produce injection volumes of approximately 1 ml. We prepared 125 μL per 25 gram weight vehicle or 10, 20, or 30 mg/kg ML314 solutions for injection in mice as follows. ML314 powder (0, 2, 4, or 6 mg) dissolved in 20 μL of 100% tissue culture grade DMSO (Sigma-Aldrich, St. Louis, MO) was mixed with 20 μL of a 100% solution of Tween-20 (Sigma-Aldrich), followed by addition of picopure (reverse osmotic, deionized) water to a final volume of 1 ml yielding a 0, 2, 4, or 6 μg/ μL solution. Due to solubility limits for ML314, after a few minutes at room temperature the solution became somewhat milky and was used in this form for i.p. injection with a 28 gauge insulin syringe. All experiments with mice were approved in a protocol by the Duke University Institutional Animal Care and Use Committee and adhere to the National Academy of Sciences' Guide for the Care and Use of Laboratory Animals.

Locomotion

Locomotor activity was measured in an Omnitech Digiscan activity monitor (20×20 cm2; Accuscan Instruments, Columbus, OH) as described 34. Locomotor activity was measured at 5 min intervals.. To evaluate the effects of compounds on locomotor behavior, the mice were placed in an activity monitor for a 20 min habituation period, and afterwards injected with drug or vehicle, returned to the monitor, and locomotor activity was recorded over a period of 90 minutes. Treatments included one of the following drugs: PD149163 (1 mg/Kg), ML314 (5 mg/Kg), YIL781 (10 mg/Kg) or a combination of 5 mg/Kg ML314 and 10 mg/Kg YIL781. In methamphetamine sensitization experiments, C57BL/6J mice were first exposed to the activity boxes for 120 min, 4 d before the test. On day 1, mice were habituated to the activity box for 30 min, meth (2 mg/kg, i.p.) was then given, and activity was recorded for

120 minutes. The same group of mice was administered methamphetamine (2 mg/kg, i.p.) once per day for the next 4 consecutive days in home cages for a total of 5 days of daily treatment. The mice were not handled or treated for the next 4 days. On day 10, the mice were treated the same as on day 1; after a 30 minute habituation, meth (1 mg/kg, i.p.) was administered with or without ML314 (10-30 mg/kg i.p.) or ML314 15 minutes prior to the meth injection and activity was monitored. Displacement data were analyzed in GraphPad Prism using a Cauchy (Lorentzian) or Gaussian distribution with offset. The Cauchy model produced either equivalent or slightly better fits in all instances.

Conditioned Place Preference

Conditioned preference was measured in a three-chamber system (model ENV-3013, Med Associates, St. Albans, VT) with the two larger end chambers used for conditioning sessions. One of the two end chambers had bar flooring and black walls, the other had grid flooring and white walls, and the gray center chamber had solid flooring. On a pretest day 0, mice were first placed in the center chamber with the doors connecting the two end chambers open. The time spent in each of the three chambers was recorded for 30 minutes. Mice were treated with an (i.p.) injection of meth (2 mg/ml) on days 1, 3, and 5 and saline on days 2, 4, and 6. The mice were confined to an assigned end chamber post-injection for 30 minutes. Each mouse was confined to either the black or white chamber when receiving meth and to the opposite chamber when given saline the following day. To ensure that the assignment was unbiased, those mice that spent more than 60% of the 30-minute preconditioning period in one end chamber were assigned to the alternate chamber for meth injection; for the mice showing no chamber bias, meth treatment was randomly paired with end chambers such that equal numbers of mice received meth in each end chamber. On the test day, mice were assigned to vehicle or ML314 treatments (20 mg/ml, i.p.). 15 minutes after an injection the mice were allowed to explore the 3 chambers freely for 30 additional minutes. Data were expressed as the time spent in either the saline- or meth-paired chamber. Preference scores are calculated as the time spent in the saline chamber subtracted from the time spent in the meth chamber and divided by the total time spent in both chambers.

Wire Hang Test

10 week old, C57BL/6J mice were used with average body weights of 25g for males and 20g for females. On day one a mouse was placed upon a wire cage top, and the cage top was gently inverted so that the animal would grasp and hang from the wire. This was permitted for up to 60 seconds at which time the training ended and the mouse was returned to the home cage. Two mice that fell within the 60 second period of l training were retrained after a 10 minute rest. All mice successfully hung onto the inverted wire top for 60 seconds. On day two, the wire-hang test was at 60 minutes after receiving an i.p. vehicle injection (2% DMSO, 2% Tween-20 in H_2O). On days three and four the test was repeated to 30 minutes and one hour respectively following a 20mg/kg ML314 (i.p.) injection. Data were expressed as the latency time in which the mouse lost its grip and fell from the wire.

Self-Administration of Meth in Rats

Sprague-Dawley rats were obtained from Charles Rivers Laboratories (Raleigh, NC). Animals were trained according to the paradigm described in Frankel et al [38]. All

experiments were approved by the University of Utah Institutional Animal Care and Use Committee and adhered to the National Academy of Sciences' Guide for the Care and Use of Laboratory Animals.

Acknowledgments

We thank Dr. J. Snyder for discussions and his critical review of this manuscript and Lauren Rochelle for her expertise in FAP technology and carrying out experiments in this area.

Funding Sources: This work was supported by NIH grants 1 R03 MH089653-01 to L.S.B., 5P30DA029925 (M.G.C., L.S.B.), R01DA031883 to G.R.H., and an NIH Molecular Libraries grant (U54 HG005033-03) to the Conrad Prebys Center for Chemical Genomics at the Sanford-Burnham Medical Research Institute, one of the comprehensive centers of the NIH Molecular Libraries Probe Production Centers Network (MLPCN).

References

1. Frankel PS, Hoonakker AJ, Alburges ME, McDougall JW, McFadden LM, Fleckenstein AE, Hanson GR. Effect of methamphetamine self-administration on neurotensin systems of the basal ganglia. J Pharmacol Exp Ther. 2011; 336:809–815. [PubMed: 21131268]
2. Roehr B. Half a million Americans use methamphetamine every week. BMJ. 2005; 331:476. [PubMed: 16141155]
3. Hser YI, Huang D, Brecht ML, Li L, Evans E. Contrasting trajectories of heroin, cocaine, and methamphetamine use. Journal of addictive diseases. 2008; 27:13–21. [PubMed: 18956525]
4. Volkow, ND. Methamphetamine, Letter from the Director. 2014. http://www.drugabuse.gov/publications/research-reports/methamphetamine/letter-director
5. Carraway R, Leeman SE. The isolation of a new hypotensive peptide, neurotensin, from bovine hypothalami. J Biol Chem. 1973; 248:6854–6861. [PubMed: 4745447]
6. Drumheller AD, Gagne MA, St-Pierre S, Jolicoeur FB. Effects of neurotensin on regional brain concentrations of dopamine, serotonin and their main metabolites. Neuropeptides. 1990; 15:169–178. [PubMed: 1701223]
7. Kalivas PW. Neurotransmitter regulation of dopamine neurons in the ventral tegmental area. Brain Res Brain Res Rev. 1993; 18:75–113. [PubMed: 8096779]
8. Ford AP, Marsden CA. In vivo neurochemical and behavioural effects of intracerebrally administered neurotensin and D-Trp11-neurotensin on mesolimbic and nigrostriatal dopaminergic function in the rat. Brain Res. 1990; 534:243–250. [PubMed: 2073584]
9. Perron A, Sarret P, Gendron L, Stroh T, Beaudet A. Identification and functional characterization of a 5-transmembrane domain variant isoform of the NTS2 neurotensin receptor in rat central nervous system. J Biol Chem. 2005; 280:10219–10227. [PubMed: 15637074]
10. Quirion R, Rowe WB, Lapchak PA, Araujo DM, Beaudet A. Distribution of neurotensin receptors in mammalian brain. What it is telling us about its interactions with other neurotransmitter systems. Ann N Y Acad Sci. 1992; 668:109–119. [PubMed: 1361109]
11. Sarret P, Perron A, Stroh T, Beaudet A. Immunohistochemical distribution of NTS2 neurotensin receptors in the rat central nervous system. J Comp Neurol. 2003; 461:520–538. [PubMed: 12746866]
12. Uhl GR. Distribution of neurotensin and its receptor in the central nervous system. Ann N Y Acad Sci. 1982; 400:132–149. [PubMed: 6301323]
13. Walker N, Lepee-Lorgeoux I, Fournier J, Betancur C, Rostene W, Ferrara P, Caput D. Tissue distribution and cellular localization of the levocabastine-sensitive neurotensin receptor mRNA in adult rat brain. Brain Res Mol Brain Res. 1998; 57:193–200. [PubMed: 9675417]
14. Matsuyama S, Higashi H, Maeda H, Greengard P, Nishi A. Neurotensin regulates DARPP-32 thr34 phosphorylation in neostriatal neurons by activation of dopamine D1-type receptors. J Neurochem. 2002; 81:325–334. [PubMed: 12064480]

15. Chalon P, Vita N, Kaghad M, Guillemot M, Bonnin J, Delpech B, Le Fur G, Ferrara P, Caput D. Molecular cloning of a levocabastine-sensitive neurotensin binding site. FEBS Lett. 1996; 386:91–94. [PubMed: 8647296]
16. Mazella J, Botto JM, Guillemare E, Coppola T, Sarret P, Vincent JP. Structure, functional expression, and cerebral localization of the levocabastine-sensitive neurotensin/neuromedin N receptor from mouse brain. J Neurosci. 1996; 16:5613–5620. [PubMed: 8795617]
17. Mazella J, Zsurger N, Navarro V, Chabry J, Kaghad M, Caput D, Ferrara P, Vita N, Gully D, Maffrand JP, Vincent JP. The 100-kDa neurotensin receptor is gp95/sortilin, a non-G-protein-coupled receptor. J Biol Chem. 1998; 273:26273–26276. [PubMed: 9756851]
18. Tanaka K, Masu M, Nakanishi S. Structure and functional expression of the cloned rat neurotensin receptor. Neuron. 1990; 4:847–854. [PubMed: 1694443]
19. Vincent JP, Mazella J, Kitabgi P. Neurotensin and neurotensin receptors. Trends in pharmacological sciences. 1999; 20:302–309. [PubMed: 10390649]
20. Vita N, Laurent P, Lefort S, Chalon P, Dumont X, Kaghad M, Gully D, Le Fur G, Ferrara P, Caput D. Cloning and expression of a complementary DNA encoding a high affinity human neurotensin receptor. FEBS Lett. 1993; 317:139–142. [PubMed: 8381365]
21. Rajagopal S, Rajagopal K, Lefkowitz RJ. Teaching old receptors new tricks: biasing seven-transmembrane receptors. Nature reviews Drug discovery. 2010; 9:373–386. [PubMed: 20431569]
22. Elde R, Schalling M, Ceccatelli S, Nakanishi S, Hokfelt T. Localization of neuropeptide receptor mRNA in rat brain: initial observations using probes for neurotensin and substance P receptors. Neurosci Lett. 1990; 120:134–138. [PubMed: 1705671]
23. Keiser AA, Matazel KS, Esser MK, Feifel D, Prus AJ. Systemic administration of the neurotensin NTS(1)-receptor agonist PD149163 improves performance on a memory task in naturally deficient male brown Norway rats. Experimental and clinical psychopharmacology. 2014; 22:541–547. [PubMed: 25222546]
24. Feifel D, Melendez G, Murray RJ, Tina Tran DN, Rullan MA, Shilling PD. The reversal of amphetamine-induced locomotor activation by a selective neurotensin-1 receptor agonist does not exhibit tolerance. Psychopharmacology (Berl). 2008; 200:197–203. [PubMed: 18568338]
25. Feifel D, Reza TL, Wustrow DJ, Davis MD. Novel antipsychotic-like effects on prepulse inhibition of startle produced by a neurotensin agonist. J Pharmacol Exp Ther. 1999; 288:710–713. [PubMed: 9918579]
26. Torup L, Borsdal J, Sager T. Neuroprotective effect of the neurotensin analogue JMV-449 in a mouse model of permanent middle cerebral ischaemia. Neurosci Lett. 2003; 351:173–176. [PubMed: 14623134]
27. Boules M, Li Z, Smith K, Fredrickson P, Richelson E. Diverse roles of neurotensin agonists in the central nervous system. Frontiers in endocrinology. 2013; 4:36. [PubMed: 23526754]
28. Richelson E, Boules M, Fredrickson P. Neurotensin agonists: possible drugs for treatment of psychostimulant abuse. Life sciences. 2003; 73:679–690. [PubMed: 12801589]
29. Caceda R, Binder EB, Kinkead B, Nemeroff CB. The role of endogenous neurotensin in psychostimulant-induced disruption of prepulse inhibition and locomotion. Schizophrenia research. 2012; 136:88–95. [PubMed: 22104138]
30. Griebel G, Holsboer F. Neuropeptide receptor ligands as drugs for psychiatric diseases: the end of the beginning? Nature reviews Drug discovery. 2012; 11:462–478. [PubMed: 22596253]
31. Barak LS, Peterson S. Modeling of bias for the analysis of receptor signaling in biochemical systems. Biochemistry. 2012; 51:1114–1125. [PubMed: 22221218]
32. Evron T, Peterson SM, Urs NM, Bai Y, Rochelle LK, Caron MG, Barak LS. G Protein and Beta-arrestin Signaling Bias at the Ghrelin Receptor. J Biol Chem. 2014
33. Hershberger, P.; Hedrick, M.; Peddibhotla, S.; Maloney, P.; Li, Y.; Milewski, M.; Gosalia, P.; Gray, W.; Mehta, A.; Sugarman, E.; Hood, B.; Suyama, E.; Nguyen, K.; Heynen-Genel, S.; Vasile, S.; Salaniwal, S.; Stonich, D.; Su, Y.; Mangravita-Novo, A.; Vicchiarelli, M.; Smith, LH.; Roth, G.; Diwan, J.; Chung, TDY.; Caron, MG.; Thomas, JB.; Pinkerton, AB.; Barak, LR. Probe Reports from the NIH Molecular Libraries Program. Bethesda (MD): 2010. Small Molecule Agonists for the Neurotensin 1 Receptor (NTR1 Agonists).

34. Hershberger PM, Hedrick MP, Peddibhotla S, Mangravita-Novo A, Gosalia P, Li Y, Gray W, Vicchiarelli M, Smith LH, Chung TD, Thomas JB, Caron MG, Pinkerton AB, Barak LS, Roth GP. Imidazole-derived agonists for the neurotensin 1 receptor. Bioorganic & medicinal chemistry letters. 2014; 24:262–267. [PubMed: 24332089]

35. Peddibhotla S, Hedrick MP, Hershberger P, Maloney PR, Li Y, Milewski M, Gosalia P, Gray W, Mehta A, Sugarman E, Hood B, Suyama E, Nguyen K, Heynen-Genel S, Vasile S, Salaniwal S, Stonich D, Su Y, Mangravita-Novo A, Vicchiarelli M, Roth GP, Smith LH, Chung TD, Hanson GR, Thomas JB, Caron MG, Barak LS, Pinkerton AB. Discovery of ML314, a Brain Penetrant Non-Peptidic beta-Arrestin Biased Agonist of the Neurotensin NTR1 Receptor. ACS medicinal chemistry letters. 2013; 4:846–851. [PubMed: 24611085]

36. Rajagopal S, Bassoni DL, Campbell JJ, Gerard NP, Gerard C, Wehrman TS. Biased agonism as a mechanism for differential signaling by chemokine receptors. J Biol Chem. 2013; 288:35039–35048. [PubMed: 24145037]

37. Clifford PS, Rodriguez J, Schul D, Hughes S, Kniffin T, Hart N, Eitan S, Brunel L, Fehrentz JA, Martinez J, Wellman PJ. Attenuation of cocaine-induced locomotor sensitization in rats sustaining genetic or pharmacologic antagonism of ghrelin receptors. Addiction biology. 2012; 17:956–963. [PubMed: 21790898]

38. Frankel PS, Hoonakker AJ, Hanson GR. Differential response of neurotensin to methamphetamine self-administration. Ann N Y Acad Sci. 2008; 1139:112–117. [PubMed: 18991855]

39. Oakley RH, Laporte SA, Holt JA, Barak LS, Caron MG. Molecular determinants underlying the formation of stable intracellular G protein-coupled receptor-beta-arrestin complexes after receptor endocytosis*. J Biol Chem. 2001; 276:19452–19460. [PubMed: 11279203]

40. Shenoy SK, Lefkowitz RJ. beta-Arrestin-mediated receptor trafficking and signal transduction. Trends in pharmacological sciences. 2011; 32:521–533. [PubMed: 21680031]

41. Schwartz TW, Holst B. Allosteric enhancers, allosteric agonists and ago-allosteric modulators: where do they bind and how do they act? Trends in pharmacological sciences. 2007; 28:366–373. [PubMed: 17629958]

42. Conn PJ, Christopoulos A, Lindsley CW. Allosteric modulators of GPCRs: a novel approach for the treatment of CNS disorders. Nature reviews Drug discovery. 2009; 8:41–54. [PubMed: 19116626]

43. Barak LS, Ferguson SS, Zhang J, Caron MG. A beta-arrestin/green fluorescent protein biosensor for detecting G protein-coupled receptor activation. J Biol Chem. 1997; 272:27497–27500. [PubMed: 9346876]

44. Snyder JC, Pack TF, Rochelle LK, Chakraborty SK, Zhang M, Eaton AW, Bai Y, Ernst LA, Barak LS, Waggoner AS, Caron MG. A rapid and affordable screening platform for membrane protein trafficking. BMC biology. 2015; 13:107. [PubMed: 26678094]

45. Zhang M, Chakraborty SK, Sampath P, Rojas JJ, Hou W, Saurabh S, Thorne SH, Bruchez MP, Waggoner AS. Fluoromodule-based reporter/probes designed for in vivo fluorescence imaging. The Journal of clinical investigation. 2015; 125:3915–3927. [PubMed: 26348895]

46. White JF, Grodnitzky J, Louis JM, Trinh LB, Shiloach J, Gutierrez J, Northup JK, Grisshammer R. Dimerization of the class A G protein-coupled neurotensin receptor NTS1 alters G protein interaction. Proceedings of the National Academy of Sciences of the United States of America. 2007; 104:12199–12204. [PubMed: 17620610]

47. Hanson GR, Hoonakker AJ, Robson CM, McFadden LM, Frankel PS, Alburges ME. Response of neurotensin basal ganglia systems during extinction of methamphetamine self-administration in rat. J Pharmacol Exp Ther. 2013; 346:173–181. [PubMed: 23685547]

48. Uhl GR, Vandenbergh DJ, Miner LL. Knockout mice and dirty drugs. Drug addiction. Current biology : CB. 1996; 6:935–936. [PubMed: 8805320]

49. Jensen PC, Thiele S, Ulven T, Schwartz TW, Rosenkilde MM. Positive versus negative modulation of different endogenous chemokines for CC-chemokine receptor 1 by small molecule agonists through allosteric versus orthosteric binding. J Biol Chem. 2008; 283:23121–23128. [PubMed: 18559339]

50. Baillie GL, Horswill JG, Anavi-Goffer S, Reggio PH, Bolognini D, Abood ME, McAllister S, Strange PG, Stephens GJ, Pertwee RG, Ross RA. CB(1) receptor allosteric modulators display

both agonist and signaling pathway specificity. Molecular pharmacology. 2013; 83:322–338. [PubMed: 23160940]

51. Lepiku M, Jarv J, Rinken A, Fuxe K. Mechanism of modulation of [3H]raclopride binding to dopaminergic receptors in rat striatal membranes by sodium ions. Neurochemistry international. 1997; 30:575–581. [PubMed: 9152999]
52. Liu W, Chun E, Thompson AA, Chubukov P, Xu F, Katritch V, Han GW, Roth CB, Heitman LH, AP IJ, Cherezov V, Stevens RC. Structural basis for allosteric regulation of GPCRs by sodium ions. Science. 2012; 337:232–236. [PubMed: 22798613]
53. Briegel A, Li X, Bilwes AM, Hughes KT, Jensen GJ, Crane BR. Bacterial chemoreceptor arrays are hexagonally packed trimers of receptor dimers networked by rings of kinase and coupling proteins. Proceedings of the National Academy of Sciences of the United States of America. 2012; 109:3766–3771. [PubMed: 22355139]
54. Fotiadis D, Jastrzebska B, Philippsen A, Muller DJ, Palczewski K, Engel A. Structure of the rhodopsin dimer: a working model for G-protein-coupled receptors. Current opinion in structural biology. 2006; 16:252–259. [PubMed: 16567090]
55. Gurevich VV, Gurevich EV. GPCR monomers and oligomers: it takes all kinds. Trends in neurosciences. 2008; 31:74–81. [PubMed: 18199492]
56. Changeux JP. Allostery and the Monod-Wyman-Changeux model after 50 years. Annual review of biophysics. 2012; 41:103–133.
57. Lodowski DT, Salom D, Le Trong I, Teller DC, Ballesteros JA, Palczewski K, Stenkamp RE. Crystal packing analysis of Rhodopsin crystals. Journal of structural biology. 2007; 158:455–462. [PubMed: 17374491]
58. Zhang Z, Melia TJ, He F, Yuan C, McGough A, Schmid MF, Wensel TG. How a G protein binds a membrane. J Biol Chem. 2004; 279:33937–33945. [PubMed: 15173184]
59. Gurevich VV, Gurevich EV. Structural determinants of arrestin functions. Progress in molecular biology and translational science. 2013; 118:57–92. [PubMed: 23764050]
60. Rodbell M. The role of hormone receptors and GTP-regulatory proteins in membrane transduction. Nature. 1980; 284:17–22. [PubMed: 6101906]
61. Rodbell M. The complex regulation of receptor-coupled G-proteins. Advances in enzyme regulation. 1997; 37:427–435. [PubMed: 9381985]
62. Kempner ES. Novel predictions from radiation target analysis. Trends in biochemical sciences. 1993; 18:236–239. [PubMed: 8212129]

Abbreviations

CPP	Conditioned place preference
DA	Dopamine
DAT	Dopa-mine Transporter
GPCR	G protein coupled receptor
i.p.	Intra-peritoneal
meth	Methamphetamine
NT	Neurotensin
NTR1	Human neurotensin receptor type 1

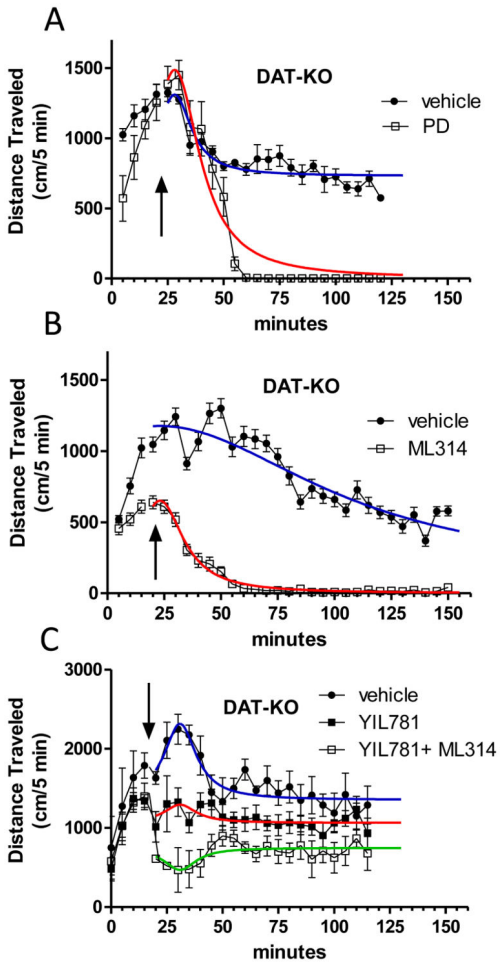

Figure 1. Locomotion of dopamine transporter knockout mice in the presence of ML314

Mice were injected (i.p.) at the times indicated by arrows with vehicle (saline) or compound, and horizontal distance traveled over 5 minute intervals measured. Points following the injection were fit to Lorentzian distributions with amplitude, center, width, and offset terms, **[*amp, cent, width, off*]**. **A.** PD at 1 mg/kg, vehicle **[*580 ± 61, 28.1 ± 0.86, 8.98 ± 2.1, 731 ± 22*]**, n= 6; PD **[*1488 ± 65, 28.1 ± 0.86, 13.5 ±, 1.5, 0 ± 0*]**, n = 4; **B.** ML314 at 20 mg/kg i.p., vehicle **[*1053 ± 88, 23.2 ± 1.0, 85.9 ± 9.3, 123 ± 94*]**, n = 7; ML314 **[*652 ± 30, 23.2 ± 1.0, 12.4 ± 1.4, 0 ± 11*]**, n = 10. **C.** YIL781 at 10 mg/kg, or YIL781 at 10 mg/kg and ML314 at 5 mg/kg, vehicle **[*964 ± 161, 30.9 ± 1.4, 8.8 ± 2.5, 1353 ± 59*]**, n = 5; YIL781 **[*231 ± 116, 30.9 ± 1.4, 8.8 ± 2.5, 1063 ± 43*]**, n = 4; YIL781 + ML314 **[*280 ± 136, 30.9 ± 1.4, 8.8 ± 2.5, 750 ± 47*]**, n = 6. Data are presented as parameter ± standard error and were fit using GraphPad Prism 5.0.

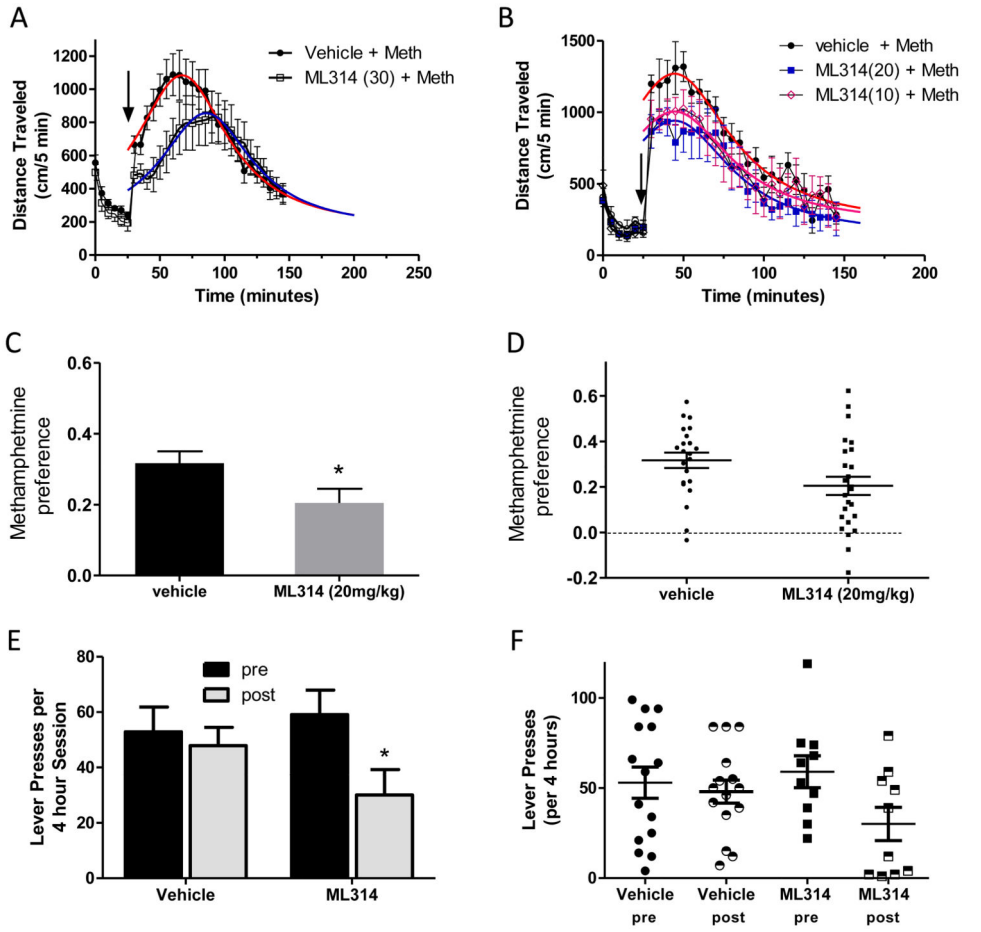

Figure 2. Effect of ML314 on horizontal locomotion and conditioned place preference in the presence of methamphetamine

A- B. Mice placed in activity monitors and were injected (i.p.) at the times indicated by arrows with vehicle (saline) or the indicated compounds plus methamphetamine at 2 mg/kg (i.p.). Horizontal distance traveled over 5 minute intervals is plotted and points following the injection were fit to Lorentzian distributions with amplitude, center, width, and offset terms, **[*amp, cent, width, off*]**. (**A**) ML314 at 30mg/kg, vehicle **[*933* ± *36, 67.1* ± *0.67, 43.4* ± *2.6, 151* ± *40.1*, n = 7; ML314 **[*705* ± *40, 85.6* ± *0.8, 43.4* ±, *2.6, 151* ± *40*]**, n = 7; **B.** ML314 at 20 and 10 mg/kg i.p., vehicle **[*1067* ± *48, 44.5* ± *1.5, 42.5* ± *3.6, 204* ± *45*]**, n = 5; ML314-20 **[*811* ± *45, 44.5* ± *1.5, 42.5* ± *3.6, 130* ± *38*]**, n = 5; ML314-10 **[*798* ± *45, 44.5* ± *1.5, 42.5* ± *3.6, 208* ± *38*]**, n = 5. Data are reported as parameter ± standard error and were determined using the program GraphPad Prism version 5.04. **C-D.** Bar graph of CPP results in (C) depicts the mean ± sem preference of WT C57BL/6J mice in the presence of vehicle (***0.32* ± *0.03***, n = 22 mice) or 20 mg/kg ML314 (***0.20* ± *0.04***, n=25 mice), Data were compared by Student's t-test using GraphPad Prism, p=0.04. Graph in (D) is a scatter plot of the responses of the cohort of mice with mean shown in (C). **E-F.** Reduction of meth self-administration by pretreatment with ML314 (30 mg/kg) or vehicle. The pre group is the total presses during the 4 hour session the day before the drug treatment. The post group is the 4 hours session after the ML314 or vehicle was injected. Either ML314 or vehicle was injected 15 minutes prior to placement of rats in a self-administration chamber. Each lever press

resulted in an i.v. infusion of 0.06 mg of meth. Results for pre/post exposure expressed as (mean ± sem, N)/ (mean ± sem, N) were for vehicle (***53.0 ± 8.3***, 15)/(***48.0 ± 6.2***, 15) and for ML314 (***59.1 ± 8.3***, 10)/(***30. 1 ± 8.7***, 10). Data were analyzed by Repeated Measures Analysis of Variance using SAS software, * corresponds to p = 0.0013. Graph in (F) is a scatter plot of the cohort responses of rats with mean shown in (E).

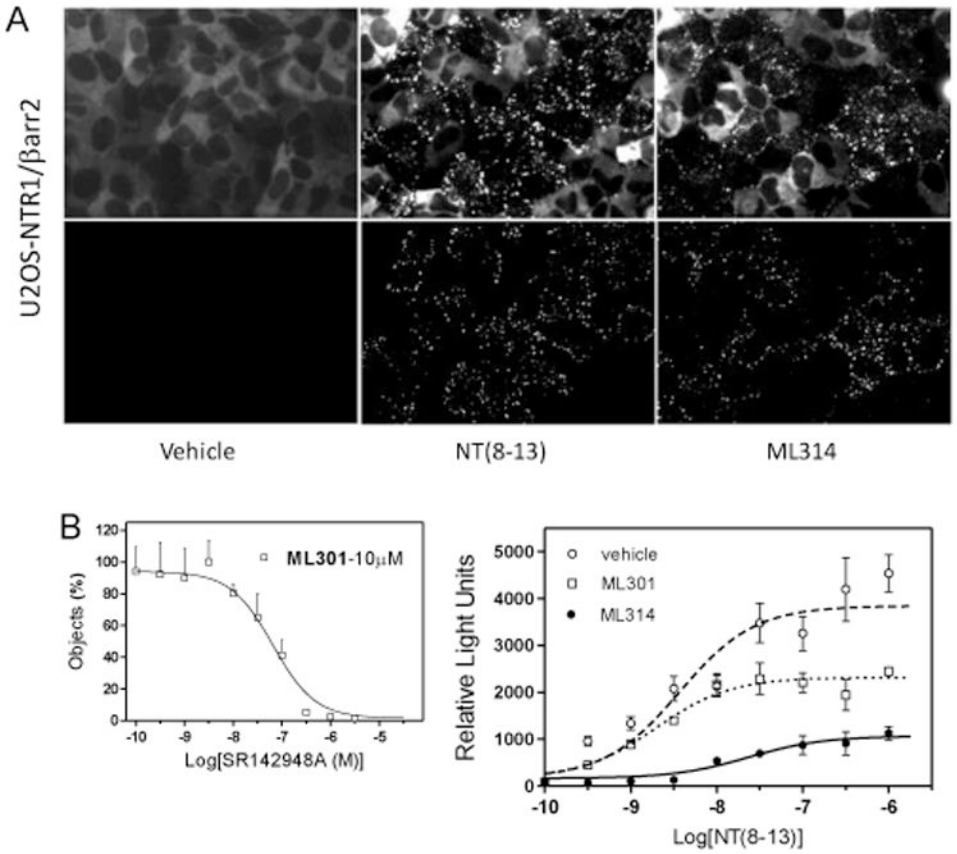

Figure 3. ML314 Activity via β-arrestin and G protein pathways

A. Fluorescence images of fixed U2OS cells (upper panels) demonstrating that translocation of β-arrestin2-GFP in a U2OS cell line containing the NTR1. Images were taken using a fluorescein filter set and a 40×, Plan Apo objective, NA/0.85, on a Zeiss Axiovert 200. To improve aggregate definition, the upper panel images were subject to wavelet analysis using the in-house, computer software Waveprog [32] to remove high frequency noise and the low frequency blur arising from non-translocated, homogeneously distributed cytoplasmic β-arrestin2-GFP (corresponding lower panels). **B.** Competitive assessment of β-arrestin2 translocation to the NTR1 using the antagonist SR142948A in U2OS cells (left). The cells were pre-treated with the neurotensin receptor antagonist SR142948A for 10 minutes as described [35], followed by the addition of 10 μM ML301 for 40 minutes and paraformaldehyde fixation. The number of cytoplasmic aggregated objects was determined using Waveprog [32]. Log(IC_{50}) for SR142948A inhibition of ML301 is ***-7.2 ± 0.13*** (mean ± sem, N = 3 independent experiments). Assessing the effects of ML314 and the control compound ML301 on NT(8-13) calcium signaling (right). HEK-293 cells expressing NTR1 were equilibrated with 5 μM Coelenterazine H for 2 hours in the dark at 37°C. Ten minutes prior to the measurement, the cells were treated with vehicle, 10 μM ML301, or 10 μM ML314. Treated cells were injected into assay plate wells containing the neurotensin peptide fragment NT(8-13), and bioluminescence was recorded for 15 seconds following injection. Data fit to a sigmoid response using GraphPad Prism version 5 and are presented as mean ±

sem. (Maxima, Log(IC50)) for NT(8-13) are in the presence of vehicle, (***3841 ± 140, -8.4 ± 0.09***); ML301, (***2316 ± 134, -8.7 ± 0.16***); ML314, (***1065 ± 206, -7.6 ± 0.43***); (N = 3).

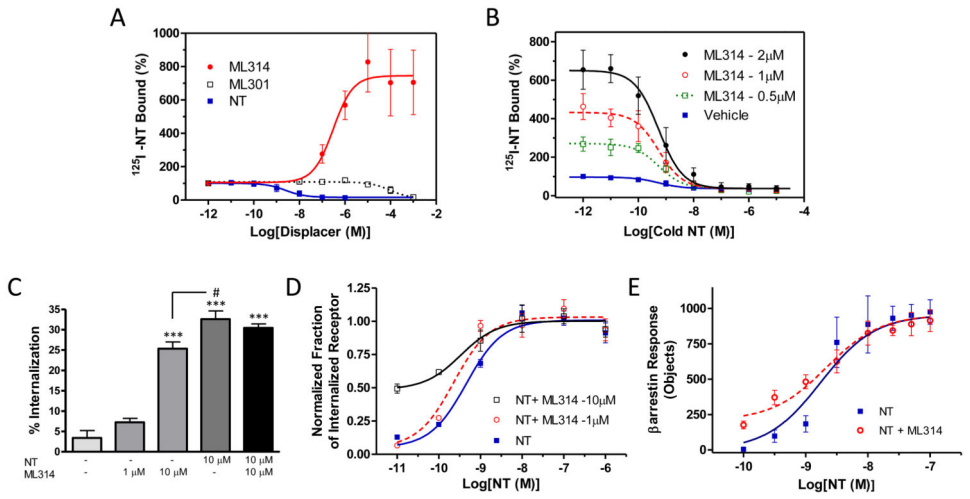

Figure 4. ML314 and Neurotensin Receptor1 NT-mediated binding, internalization, and β-arrestin translocation

A. The competitive displacement of ^{125}I-NT was measured in the presence of ML314, ML301, or cold NT. Membranes containing the NTR1 were incubated in 100 μL of binding buffer at room temperature in the presence of 10 pM ^{125}I-NT and increasing concentrations of neurotensin (NT) peptide, ML301, or ML314. Dose response curves of displacing compound were acquired and data are expressed as percent bound radioligand (mean ± sem) relative to no displacer (100%). The percent remaining with large concentrations of displacer and Log(IC50)s are for the different compounds: NT, (16 ± 8 %, -8.6 ± 0.3); ML301, (9 ± 13 %, -4.0 ± 0.2); ML314, (745 ± 123 %, -6.5 ± 0.45); (N = 3). **B.** The competitive displacement of ^{125}I-NT by cold NT from the NTR1 in the presence of different doses of ML314 was measured in U2OS cell membranes. Percent bound radioligand relative to vehicle (100%) was determined as in (A). Data were fit to a shared Log(IC50), -9.3 ± 0.09, and shared minimum of the sigmoid response curve, 37 ± 9. Computed curve maxima are: NT, 96 ± 22 %; ML314 (0.5 μM, 1 μM 2 μM), (271 ± 22 %, 433 ± 23 %, 651 ± 24 %); (N = 3). **C-D.** U2OS cells transfected with the FAP-NTR1 were simultaneously treated with NT, ML314, and/or vehicle at time 0, and remaining plasma membrane receptor was compared to untreated controls at 1 hour using the FAP-based assay (Methods). (C) Data were analyzed by 1 way ANOVA with Tukey's multiple comparison test and results are reported as mean ± sem from N =4 independent experiments done in triplicate except where noted. In order from left to right the bar heights are: (3.4 ± 1.8 %, N=2; 7.2 ± 1.0 %; 25.3 ± 1.7 %; 32.6 ± 2.0 %; 30.4 ± 1.0 %), *** $p < 0.001$ and # $p < 0.05$. (D) Data points represent mean ± sem were fit using nonlinear regression to a sigmoid curve with a constraint that the "bottom" values of the NT (■) and NT + ML314-1 μM (○) fitted curves are shared. Top, bottom, and Log(EC 50) values for each curve were NT (1.01 ±.04, 0.050 ±.045, -9.34±0.13), ML314-1 μM (1.03 ±.04, 0.050 ±.045, -9.64±0.13), and NT ML314-10μM (1.00 ±.07, 0.49 ±.07, -9.48±0.29). Data represent N=4 independent experiments performed in triplicate. **E.** β-arrestin2-GFP translocation to NTR1 in U2OS cells was determined in the absence and presence of 10-20 μM ML314 that was added simultaneously with NT. Data points represent mean ± sem from N=4 independent experiments in duplicate NT alone)/ quadruplicate (NT and ML314) and were fit as in (D) with shared "top". Top, bottom, and

Log(EC 50) values for each curve are: NT (952 ± 37, -111 ± 105, -8.87 ± 0.17) and NT+ ML314 (952 ± 37, 206 ± 69, -8.68 ± 0.18). Data were analyzed and plotted using the software GraphPad Prism version 5.

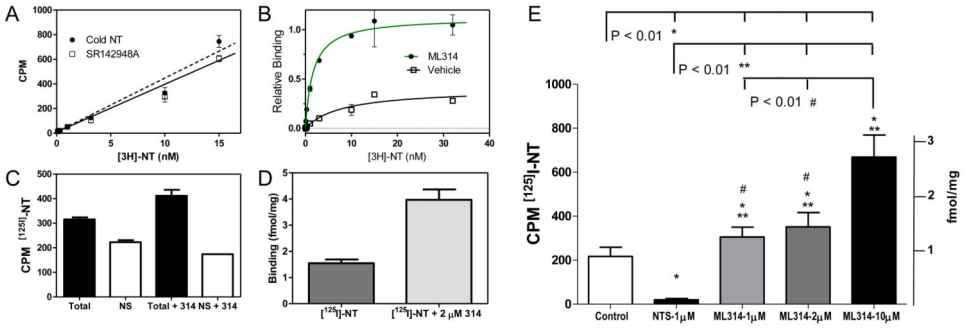

Figure 5. Increase in Membrane Binding in the presence of ML314

A. U2OS cell membranes containing the NTR1 were incubated at room temperature in the presence of vehicle or 2 μM ML314, and increasing concentrations of ^{3}H-NT peptide. Comparison of the nonspecific binding in the presence of 2 μM ML314 calculated with 1 μM cold NT peptide or 1 μM SR142948A. The (slopes per nM, intercepts) are: for cold NT, (***44 ± 3, 10 ± 2***) and for SR142948A, (***39 ± 2, 10 ± 2***); (mean ± sem, N=4). **B.** Relative specific binding for U2OS membranes calculated as total minus nonspecific binding where nonspecific binding was determined in the presence of 1 μM cold NT peptide. Calculated Bmax, Kd, and Hill slope are: **Vehicle** (***0.40 ± 0.08, 8.1 ± 3.6 nM***, 1); ML314 (***1.12 ± 0.04, 1.7 ± 0.2 nM***, 1), (mean ± sem, N = 5). **C-D.** These panels are representative of ^{125}I-NT specific binding to striatal membranes of DAT-KO mice. Tissue extracts from mouse brains were incubated in the presence of 10 pM ^{125}I-NT and with vehicle or ML314 to determine total binding. Non-specific (NS) binding was measured in the presence of cold NT peptide. Specific binding was then determined as Total minus NS. **E.** Brain membranes (100 μg/well) obtained from the striatum of DAT knockout mice were incubated in the presence of either 1 μM cold NT or the indicated concentrations of ML314 at room temperature for 10 min, at which time 10 pM of ^{125}I-NT was added for 90 minutes. The ordinate axis in counts per minute (CPM) represents specifically bound ^{125}I-NT. In each experiment the assays were conducted in quadruplicate and data are expressed as the mean ± sem (N = 4 separate experiments) and were analyzed using one-way ANOVA with Tukey's multiple comparison post-hoc test. Curve fitting and statistical analyses were performed using GraphPad Prism V5.04.

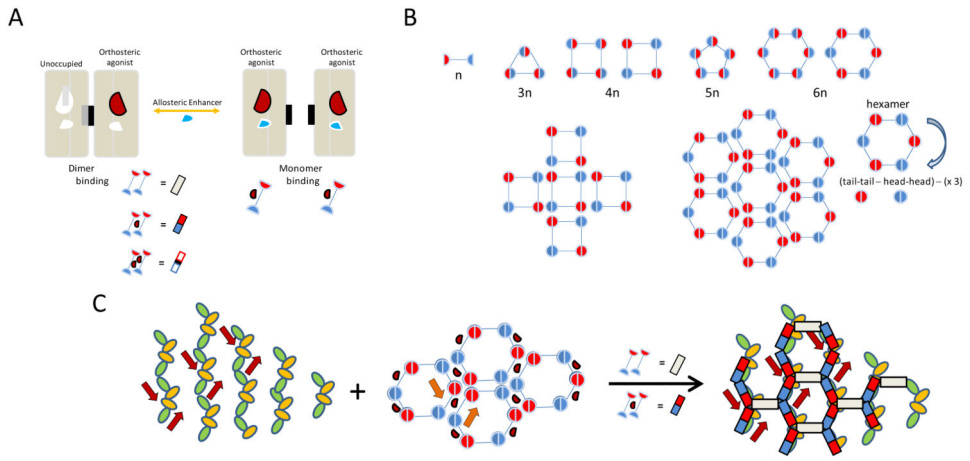

Figure 6. Symmetry modeling of ML314 induced increases in the efficacy of binding of NT to the NTR1

A. *Effect on Receptor dimers* – While receptor dimers should have three possible choices in binding an orthosteric ligand (brown), compounds may be limited to binding receptor dimer protomers with a 1:1 stoichiometry (1 ligand per 2 receptor monomers). The addition of an ML314 like compound (blue) would enhance ligand binding at the orthosteric site by shifting the receptor equilibrium to the dissociated monomer form. The allosteric ligand may or may not dissociate while each monomer now is free to bind NT ligand with a 1:1 stoichiometry. **B.** *Construction of symmetric protomer arrays* – The fundamental monomer building block of the array forms closed polygonal cells in which elements are connected repeatedly either tail-head-tail or tail-tail and head-head. For an odd number of elements only tail-head-tail assemblies are possible. Additionally, cells have the orientation illustrated by the arrow for the hexamer cell on the right. Examples of tail-tail, head-head lattices of cells with rotational symmetry are shown for tetramer and hexamer building blocks. **C.** *An oligomer arrangement of NTR1 protomer dimers into a hexamer based lattice* - Approximating the sides of adjacent cells creates a symmetric array of protomer dimers. Lattices of linear polarized G proteins (left, opposing arrows indicate monomer directionality) interact with and break the symmetry of a receptor hexamer array of receptor/protomer dimers (middle) to form a hexagonal lattice of receptors polarized along the direction of the G protein lattice (right). Only two of three potential receptor dimer binding regions, the ones that are aligned along the G protein axis, can be occupied by either one or two ligands. This model predicts that for a hexagonal lattice in the presence and absence of an ML314 like compound that dissociates the dimers, the occupancy ratio of bound orthosteric ligand, Bmax (with ML314 like compound)/Bmax (without ML314 like compound), is either 3 or 1.5 (bound ligand increases from either 4 of 12 or 8 of 12 to 12 of 12 sites occupied in the dissociated receptors).